photonics

MDPI

Communication

Disturbance-Observer-Based LQR Tracking Control for Electro-Optical System

Chao Liu [1,2,3,4], Yao Mao [1,2,3,*] and Xiaoxia Qiu [1,2]

1 Institute of Optics and Electronics, Chinese Academy of Sciences, Chengdu 610209, China; liuchao191@mails.ucas.ac.cn (C.L.); qiuxiaoxia19@mails.ucas.ac.cn (X.Q.)
2 University of Chinese Academy of Sciences, Beijing 100049, China
3 Key Laboratory of Optical Engineering, Chinese Academy of Sciences, Chengdu 610209, China
4 The School of Electronics, Electrical and Communication Engineering, Beijing 101408, China
* Correspondence: maoyao@ioe.ac.cn

Abstract: To improve the dynamic property and the disturbance suppression ability of an electro-optical tracking system, this paper presents a disturbance-observer-based LQR tracking control method. The disturbance-observer-based robust controller is composed of three parts: one is the LQR tracking controller, one is the reference model controller and the other is a compensatory controller designed with the output of the disturbance observer. The uncertainty and disturbances are considered in the controller design. By Lyapunov stability theory and linear matrix inequality (LMI) technique, the sufficient conditions for observer gain and controller gain of the tracking reference model of the electro-optical system are given. Simulation and experimental results show that the proposed method in this paper not only improved the disturbance suppression ability of the electro-optical tracking system but also improved the dynamic property of the electro-optical tracking system, such as rise time, settling time and system overshoot. Specially, compared with other methods in this paper, the tracking accuracy and the disturbance suppression ability of the proposed method are about two to three times higher. The method presented in this paper has important reference value in the field of electro-optical system applications. But, with the development of electro-optical system applications, the tracking accuracy and disturbance suppression ability of the proposed method cannot meet the actual requirements of an electro-optical system. The next step of this paper will consider a variety of practical requirements, such as the controller saturation problem and tracking reference target with strong maneuverability, and further optimize the proposed method.

Keywords: disturbance-observer-based control (DOBC); LQR; LMI technique; Lyapunov stability theory; electro-optical tracking platform

Citation: Liu, C.; Mao, Y.; Qiu, X. Disturbance-Observer-Based LQR Tracking Control for Electro-Optical System. *Photonics* **2023**, *10*, 900. https://doi.org/10.3390/photonics10080900

Received: 27 June 2023
Revised: 21 July 2023
Accepted: 27 July 2023
Published: 3 August 2023

1. Introduction

The electro-optical tracking platform is a complex and high-precision directional tracking system integrating optical, mechanical and electrical properties. It is widely used in long-distance laser communication, quantum communication, inertial measurement unit and other fields [1–4]. The electro-optical tracking platform is mainly used to realize real-time precision tracking and measuring of moving targets. However, it is often affected by external disturbances and internal uncertainties in engineering control applications. These disturbances seriously affect the stability performance and control effect of the system and may even cause instability of the closed-loop system. Therefore, many researchers are devoted to dealing with the disturbance and internal uncertainty of electro-optical tracking systems [5–7]. In general, the aforementioned disturbance suppression methods of electro-optical tracking platforms can be classified into the following two categories. The first category is a multiloop feedback control system composed of high-sampling-rate inertial sensors, such as the micro-electro-mechanical system (MEMS) accelerometers, fiber optical gyroscopes (FOG) and high-resolution position detectors. The disturbance suppression capabilities of the multiloop feedback control system is the superposition of the effects of each loop, but this method is insufficient for disturbance suppression capacity or dealing with internal uncertainty, and it can only provide basic disturbance suppression [8,9]. More seriously, when suffering from strong disturbances, the controlled variables might have too large fluctuations, which could even lead to instability of the closed-loop system. The second category mainly uses the direct feedforward method based on measurement to suppress disturbance. This method requires accurate identification of disturbance transfer characteristics outside the system. However, it is hard or even impossible to measure the disturbances in many actual processes, including the inertial uncertainty. Therefore, it is of practical interest to improve the disturbance rejection ability of the stable control platform to be able to observe and compensate for the disturbance source [10].

Based on the above situation and to further improve the disturbance suppression ability of the system, disturbance-observer-based control (DOBC) is introduced into the electro-optical tracking system in this paper. And this method, based on DOBC, does not require accurate model information [11,12]. In practical applications, the electro-optical tracking system requires motion tracking of the position, velocity or acceleration curve of a given time series with a certain precision. Meanwhile, the electro-optical tracking system must also meet certain control performance indicators, such as minimum tracking time and minimum cost. In this way, the system can track the specified trajectory faster, more accurately and more effectively. As we know, there is little research on the optimal tracking control of electro-optical tracking systems subject to external disturbances. At present, various optimal control methods are popular in the control field, including linear quadratic regulator optimal control (LQR), adaptive dynamic programming control [13,14], etc., to achieve ideal dynamic and steady-state performance.

The LQR is a well-known design technique in modern optimal control theory and has been widely used in many applications [15,16]. In contrast with pole placement, the desired performance objectives are directly addressed by minimizing a quadratic function of the state and control input. The resulting optimal control law has many excellent properties, including closed-loop stability. Furthermore, the trade-off between state regulatory requirements and control energy consumption in the LQR can be controlled by choosing the weighting matrices $\boldsymbol{Q}$ and $\boldsymbol{R}$ [17–19]. However, the solution to the LQR problem depends on solving the Riccati equation. Before solving the Riccati equation, designers often need to determine some undetermined parameters in advance. The selection of these parameters will not only affect the quality of the conclusion but also affect the solvability of the problem, which brings great conservatism to the solution of the problem. Meanwhile, there are still some problems in solving the Riccati equation itself. At present, there are many methods for solving the Riccati equation, but most of them are iterative methods, and the convergence of these methods cannot be guaranteed.

In view of the above problems, linear matrix inequality (LMI) technology can be well solved [20,21]. One advantage of using LMI is that it makes it easy to include other specifications for controller design [22,23]. Therefore, various design specifications can be rewritten into the LMI, and the resulting LMI constraints can be efficiently solved using newly developed convex optimization algorithms.

In this paper, a LQR-DOB tracking control method to achieve the optimal tracking of the desired trajectory under the condition of modeling error and uncertain disturbance is proposed. In summary, the contribution of this paper is as follows:

1. This paper proposes the LQR-DOB tracking control method, which solves the uncertainty of the model and the instability of the system caused by uncertain disturbance;
2. Using standard techniques, the DOB gain and LQR controller gain of the tracking reference model design is reduced to a convex constraint problem, which can be efficiently solved with the LMI approach;
3. The stability constraint of the electro-optical tracking closed-loop system is considered by using Lyapunov theory in the LMI framework;

4. Compared with other control methods, the disturbance suppression ability and dynamic response performance of the system, such as rise time, settling time and system overshoot, have been significantly improved under the proposed method.

The rest of this paper is organized as follows. In Section 2, the electro-optical tracking platform is modeled. In Section 3, the LQR-DOB tracking controller is designed and analyzed. In Section 4, the simulated and experimental results are presented. In Section 5, the direction of future work is pointed out. Finally, Section 6 concludes the paper.

2. Modeling of The Electro-Optical Tracking Platform

The main structure of the electro-optical tracking stable platform is shown in Figure 1a. A detector such as PSD receives the beacon of light reflected by the tip-tilt mirror and sends the position error signal to the controller. The controller calculates the correction angle of the mirror, and then through the D/A converter, the output of the controller drives the motors connected to the mirror. The aim is to stabilize the light at the center of the detector by rapidly deflecting the mirror under the influence of the disturbance.

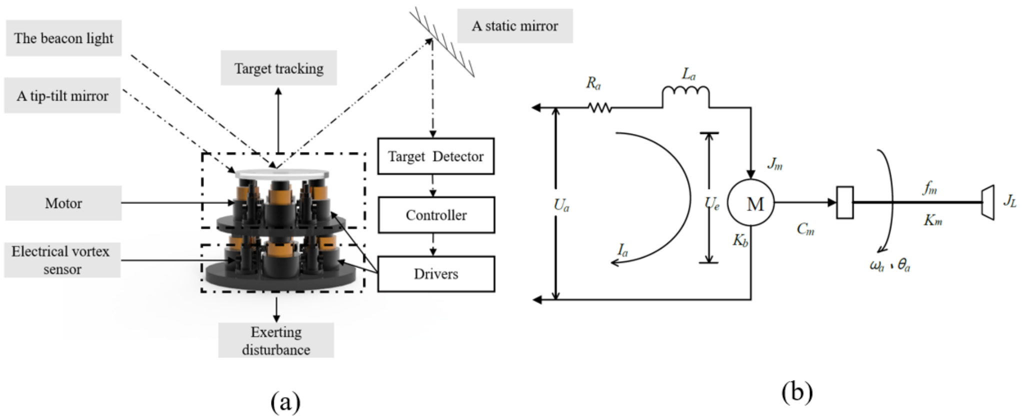

Figure 1. (**a**) The schematic of the electro-optical tracking system. (**b**) The physical model structure of the plant.

Mathematical modeling is the foundation of control. In Figure 1b, using the potential plus the torque balance equation, we obtain

$$\begin{cases} U_a = R_a I_a(s) + L_a s I_a(s) + K_b s \theta_a(s) \\ C_m I_a = (J_L s^2 + f_m s + K_m)\theta_a(s) \end{cases}, \tag{1}$$

where $U_a, I_a, R_a, L_a, K_b, C_m, f_m, K_m$ are the motor voltage, current, resistance, inductor, back electromotive force coefficient, torque coefficient, viscous friction and spring stiffness, respectively. Meanwhile, J_L, θ_a are the load inertia and the relative position angle of the motor-driven tilt mirror, respectively. Then, the controlled system plant can be modeled as

$$G(s) = \frac{\theta_a(s)}{U_a(s)} = \frac{C_m}{(J_L s^2 + f_m s + K_m)(L_a s + R_a) + K_b C_m s}. \tag{2}$$

Moreover, it can also be factorized with the typical resonance element and inertia element, which is

$$G(s) = \frac{\theta_a(s)}{U_a(s)} = \frac{K}{(s^2 + as + b)} \frac{1}{(Ts + 1)}, \tag{3}$$

where $a = 2\zeta_{ol}\omega_{ol}, b = \omega_{ol}^2$. ζ_{ol}, ω_{ol} are the damping ratio and natural frequency of the open-loop system, respectively. K is the system open-loop gain. And T is the parasitic time constant.

Since the inertia element in the controlled plant only affects the characteristics of the high-frequency part of the electro-optical tracking platform, the frequency characteristics from the voltage input U_a to the angle output θ_a can be approximated to a typical resonance element. Therefore, the general form of the controlled system object for low and intermediate frequencies can be expressed as

$$G(s) = \frac{\theta_a(s)}{U_a(s)} = \frac{K}{s^2 + as + b}, \tag{4}$$

where the meanings of a, b and K are consistent with those in Equation (3). Convert the controlled system object in Equation (4) into state-space equation form as

$$\begin{cases} \begin{bmatrix} \dot{x}_1(t) & \dot{x}_2(t) \end{bmatrix}^T = \boldsymbol{A_1}\begin{bmatrix} x_1(t) & x_2(t) \end{bmatrix}^T + \boldsymbol{B_1}u(t) \\ y = \boldsymbol{C_1}\begin{bmatrix} x_1(t) & x_2(t) \end{bmatrix}^T + \boldsymbol{D_1}u(t) \end{cases}, \tag{5}$$

where $\boldsymbol{A_1} = \begin{bmatrix} 0 & 1 \\ -b & -a \end{bmatrix}, \boldsymbol{B_1} = \begin{bmatrix} 0 \\ K \end{bmatrix}, \boldsymbol{C_1} = \begin{bmatrix} 1 & 0 \end{bmatrix}, \boldsymbol{D_1} = 0, x_1(t) = y, x_2(t) = v$; y, v represent the position and speed of the system, respectively. However, in the actual working environment, the electro-optical tracking platform will not only be affected by external interference but its characteristics will also change with the change in attitude and load. Therefore, the electro-optical tracking system in Equation (5) can be converted into

$$\begin{cases} \dot{\boldsymbol{x}}(\boldsymbol{t}) = (\boldsymbol{A_1} + \boldsymbol{\Delta A_1})\boldsymbol{x}(\boldsymbol{t}) + \boldsymbol{B_1}[u(t) + d(t)] + \boldsymbol{D_1}w(t) \\ \boldsymbol{z}(\boldsymbol{t}) = \boldsymbol{C_1}\boldsymbol{x}(\boldsymbol{t}) \end{cases}, \tag{6}$$

where $\boldsymbol{x}(\boldsymbol{t})$ denotes system state variable; $u(t)$ stands for the control input; $\boldsymbol{z}(\boldsymbol{t})$ is the controlled output; $\boldsymbol{\Delta A_1}$ denotes the parameter uncertainty; and $d(t)$ and $w(t)$ are the disturbances, where $w(t)$ is square integrable on $[\ 0, \ \ +\infty\ )$.

3. The LQR-DOB Tracking Controller

In this section, the LMI-LQR-DOB tracking controller is designed for the electro-optical tracking system with uncertainty and disturbance. The main objective of this work is to design a controller ensuring that the electro-optical tracking system can track the reference signal generated by the following model

$$\begin{cases} \dot{\boldsymbol{x}}_{\boldsymbol{r}}(\boldsymbol{t}) = \boldsymbol{A_r}\boldsymbol{x_r}(\boldsymbol{t}) + \boldsymbol{B_r}r(t) \\ \boldsymbol{z_r}(\boldsymbol{t}) = \boldsymbol{C_1}\boldsymbol{x_r}(\boldsymbol{t}) \end{cases}, \tag{7}$$

where $\boldsymbol{x_r}(\boldsymbol{t})$ denotes the state vector of the reference system, and $r(t)$ is the bounded reference input. $\boldsymbol{A_r}$, $\boldsymbol{B_r}$, $\boldsymbol{C_1}$ are known constant matrices, and $\boldsymbol{A_r}$ is Hurwitz.

The following assumptions, lemmas and definition are adopted throughout this work.

Assumption 1 ([24])**.** *The system satisfies the controllable and observable condition, that is,* $(\boldsymbol{A_1}, \boldsymbol{B_1})$ *is controllable and* $(\boldsymbol{A_1}, \sqrt{\boldsymbol{Q}})$ *is observable.*

Assumption 2 ([24])**.** *There exist two matrices* $\boldsymbol{K_1}$,$\boldsymbol{K_2}$ *such that* $\boldsymbol{A_r}, \boldsymbol{B_r}$ *in the reference model in Equation (7) satisfies* $\boldsymbol{A_r} = \boldsymbol{A_1} + \boldsymbol{B_1}\boldsymbol{K_1}$ *and* $\boldsymbol{B_r} = \boldsymbol{B_1}\boldsymbol{K_2}$.

Assumption 3 ([25])**.** *The uncertainty* ΔA_1 *can be expressed as* $\Delta A_1 = D_2 F_1(t) E_1$, *where* D_2, E_1 *are known constant matrices, and* $F_1(t)$ *is an unknown matrix satisfying* $\|F_1(t)\| \le 1$.

Lemma 1 ([26])**.** *Assume that* $\boldsymbol{X}$ *and* $\boldsymbol{Y}$ *are vectors or matrices with appropriate dimension. The following inequality*

$$\boldsymbol{X^T Y} + \boldsymbol{Y^T X} \le \alpha \boldsymbol{X^T X} + \alpha^{-1}\boldsymbol{Y^T Y}, \tag{8}$$

holds for any constant $\alpha > 0$.

Lemma 2 ([26])**.** *Assume that $\boldsymbol{H_1}$ and $\boldsymbol{H_2}$ are symmetric matrices, $\boldsymbol{S_1}$ and $\boldsymbol{S_2}$ are vectors or matrices with appropriate dimension and $\boldsymbol{F^TF} \leq \boldsymbol{I}$. The following inequality*

$$\begin{bmatrix} \boldsymbol{H_1} & \boldsymbol{S_1^T F S_2} \\ * & \boldsymbol{H_2} \end{bmatrix} \leq \begin{bmatrix} \boldsymbol{H_1} + \varepsilon \boldsymbol{S_1^T S_1} & 0 \\ 0 & \boldsymbol{H_2} + \frac{1}{\varepsilon} \boldsymbol{S_2^T S_2} \end{bmatrix}, \tag{9}$$

holds for any constant $\varepsilon > 0$.

Notations: The symmetric term is denoted as $*$, i.e., $\begin{bmatrix} \boldsymbol{X} & \boldsymbol{Y} \\ \boldsymbol{Y^T} & \boldsymbol{Z} \end{bmatrix} = \begin{bmatrix} \boldsymbol{X} & \boldsymbol{Y} \\ * & \boldsymbol{Z} \end{bmatrix}$.

Proof. Premultiplying and postmultiplying simultaneously by $\begin{pmatrix} x_1 & x_2 \end{pmatrix}$ and $\begin{pmatrix} x_1 & x_2 \end{pmatrix}^T$ with $\begin{bmatrix} \boldsymbol{H_1} & \boldsymbol{S_1^T F S_2} \\ * & \boldsymbol{H_2} \end{bmatrix}$ yields

$$x_1^T(t)\boldsymbol{H_1}x_1(t) + x_1^T(t)\boldsymbol{S_1^T F S_2}x_2(t) + x_2^T(t)\boldsymbol{S_2^T F^T S_1}x_1(t) + x_2^T(t)\boldsymbol{H_2}x_2(t). \tag{10}$$

□

According to Lemma 2 and Equation (10), for $\boldsymbol{F^T F} \leq \boldsymbol{I}$, we have

$$\begin{array}{l} x_1^T(t)\boldsymbol{H_1}x_1(t) + x_1^T(t)\boldsymbol{S_1^T F S_2}x_2(t) + x_2^T(t)\boldsymbol{S_2^T F^T S_1}x_1(t) + x_2^T(t)\boldsymbol{H_2}x_2(t) \\ \leq x_1^T(t)\left(\boldsymbol{H_1} + \alpha \boldsymbol{S_1^T S_1}\right)x_1(t) + x_2^T(t)\left(\boldsymbol{H_2} + \alpha^{-1}\boldsymbol{S_2^T S_2}\right)x_2(t) \\ = \left(x_1^T(t)x_2^T(t)\right)\begin{pmatrix} \boldsymbol{H_1} + \alpha \boldsymbol{S_1^T S_1} & 0 \\ 0 & \boldsymbol{H_2} + \alpha^{-1}\boldsymbol{S_2^T S_2} \end{pmatrix}\begin{pmatrix} x_1(t) \\ x_2(t) \end{pmatrix} \end{array}. \tag{11}$$

Combining Equations (10) and (11), we have Equation (9).

Lemma 3. *Schur complement [25]: For a given symmetric matrix $\boldsymbol{S} = \begin{bmatrix} \boldsymbol{S_{11}} & \boldsymbol{S_{12}} \\ \boldsymbol{S_{21}} & \boldsymbol{S_{22}} \end{bmatrix}$, where $\boldsymbol{S_{11}}$ is $r \times r$ dimensional and $\boldsymbol{S_{22}}$ is $(n-r) \times (n-r)$ dimensional. The following three conditions are equivalent:*

(i) $\boldsymbol{S} < \boldsymbol{0}$;

(ii) $\boldsymbol{S_{11}} < \boldsymbol{0}, \boldsymbol{S_{22}} - \boldsymbol{S_{12}^T S_{11}^{-1} S_{12}} < \boldsymbol{0}$;

(iii) $\boldsymbol{S_{22}} < \boldsymbol{0}, \boldsymbol{S_{11}} - \boldsymbol{S_{12} S_{22}^{-1} S_{12}^T} < \boldsymbol{0}$.

Defining the tracking error as $e_x(t) = x(t) - x_r(t)$ and invoking equations in Equations (6) and (7), we have

$$\dot{e}_x(t) = (\boldsymbol{A_1} + \boldsymbol{\Delta A_1})\boldsymbol{x(t)} + \boldsymbol{B_1}[u(t) + d(t)] - \boldsymbol{A_r x_r(t)} - \boldsymbol{B_r}r(t) + \boldsymbol{D_1}w(t). \tag{12}$$

The controller $u(t)$ in Figure 2 is designed as

$$u(t) = u_f(t) + u_l(t) - \hat{d}(t), \tag{13}$$

where $u_f(t)$ is the reference model matching controller, $u_l(t)$ is an LQR tracking controller and $\hat{d}(t)$ is the estimation of disturbance $d(t)$.

The reference model matching controller is given by

$$u_f(t) = K_1 x_r(t) + K_2 r(t), \tag{14}$$

where K_1, K_2 are the gain matrices satisfying Assumption 2. Substituting Equations (13) and (14) into Equation (12), we obtain

$$\dot{e}_x(t) = (\boldsymbol{A_1} + \boldsymbol{\Delta A_1})e_x(t) + \boldsymbol{B_1 u_l} + \boldsymbol{B_1}e_d(t) + \boldsymbol{\Delta A_1 x_r(t)} + \boldsymbol{D_1}w(t), \tag{15}$$

where $e_d(t) = d(t) - \hat{d}(t)$ is the disturbance error vector.

The LQR tracking controller $u_l(t)$ is designed for the following error system:

$$\dot{e}_x(t) = (\boldsymbol{A_1} + \boldsymbol{\Delta A_1})e_x(t) + \boldsymbol{B_1}u_l. \tag{16}$$

For the error tracking system in Equation (16) above, we consider an auxiliary function as

$$J(t) = \int_0^\infty \left[e_x^{\mathrm{T}}(t)\left(\boldsymbol{Q} + \boldsymbol{K}^{\mathbf{T}}\boldsymbol{RK}\right)e_x(t)\right]dt, \tag{17}$$

which is selected to design the LQR tracking controller $u_l(t)$, where $\boldsymbol{Q}$ is the semipositive definite state weighting matrix, $\boldsymbol{R}$ is the positive definite control weighting matrix and $\boldsymbol{K}$ is the gain of the LQR tracking controller.

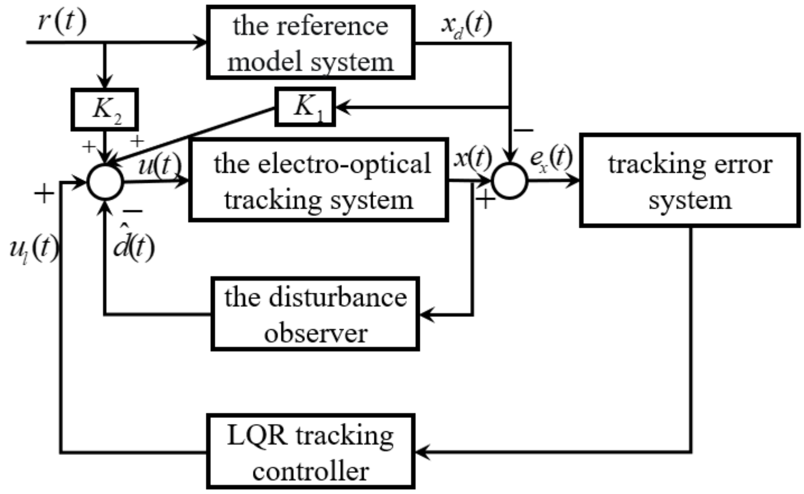

Figure 2. Block diagram of LQR-DOB tracking control.

The LQR tracking controller $u_l(t)$ is designed as

$$u_l(t) = \boldsymbol{K}e_x(t). \tag{18}$$

The above LQR tracking controller design problem can be expressed as the following optimization problem by LMI technology:

$$\min J = \int_0^\infty \left[e_x^{\mathrm{T}}(t)\left(\boldsymbol{Q} + \boldsymbol{K}^{\mathbf{T}}\boldsymbol{RK}\right)e_x(t)\right]dt < \gamma, \tag{19}$$

where γ is the upper bound of the LQR performance index. Under the condition that Assumption 1 is satisfied, the above LQR tracking controller design problem is transformed into the following inequality relationship:

$$(\boldsymbol{A_1} + \boldsymbol{\Delta A_1})\boldsymbol{x} + \boldsymbol{x}(\boldsymbol{A_1} + \boldsymbol{\Delta A_1})^{\boldsymbol{T}} + \boldsymbol{B_1W} + (\boldsymbol{B_1W})^{\mathbf{T}} + x_0x_0^{\mathrm{T}} < 0, \tag{20}$$

$$\mathrm{trace}(\sqrt{\boldsymbol{Q}}\boldsymbol{X}(\sqrt{\boldsymbol{Q}})^{\boldsymbol{T}}) + \mathrm{trace}(\boldsymbol{Y}) < \gamma, \tag{21}$$

$$\begin{bmatrix} -\boldsymbol{Y} & \sqrt{\boldsymbol{R}}\boldsymbol{W} \\ (\sqrt{\boldsymbol{R}}\boldsymbol{W})^{\boldsymbol{T}} & -\boldsymbol{X} \end{bmatrix} < 0, \tag{22}$$

where $\boldsymbol{X} \in S^n$, S^n is the set of symmetric positive definite matrices; $\boldsymbol{Y} \in S^r$, S^r is also the set of symmetric positive definite matrices; $\boldsymbol{W} \in R^{r\times n}$, $R^{r\times n}$ is the set of $r \times n$ matrices; and x_0 is the initial value of state variable x, and the trace operator is defined as $trace(\boldsymbol{S}) = \sum\limits_{i=1}^{n} s_{ii}$ with $\boldsymbol{S} = (s_{ij})_{n\times n}$.

By substituting the uncertainty $\boldsymbol{\Delta A_1}$ in Assumption 3 into Equation (20) and using Lemma 3: (Schur Complement), we can further convert Equation (20) to

$$\begin{bmatrix} A_1X + XA_1^T + B_1W + (B_1W)^{\mathrm{T}} + \alpha D_2D_2^T + x_0x_0^{\mathrm{T}} & XE_1^T \\ * & -\alpha I \end{bmatrix} < 0. \tag{23}$$

Combining Equations (21)–(23), the gain of LQR tracking controller can be determined by setting

$$K = WX^{-1}. \tag{24}$$

Then, we design the disturbance observer as

$$\begin{cases} \hat{d}(t) = \sigma(t) + Lx(t) \\ \dot{\sigma}(t) = -L[A_1x(t) + B_1u(t) + B_1\hat{d}(t)] \end{cases}, \tag{25}$$

where $\hat{d}(t)$ is the estimation of $d(t)$, $\sigma(t)$ denotes the auxiliary variable of the designed observer and L is the disturbance observer gain. The disturbance error system has the following form:

$$\begin{aligned} \dot{e}_d(t) &= \dot{d}(t) - \dot{\sigma}(t) - L\dot{x}(t) = -LB_1e_d(t) - L\Delta A_1x(t) - LD_1w(t) + \dot{d}(t) \\ &= -LB_1e_d(t) - L\Delta A_1e_x(t) - LD_1w(t) + \dot{d}(t) - L\Delta A_1x_r(t). \end{aligned}, \tag{26}$$

Combining Equations (7), (12) and (19), we have

$$\begin{cases} \dot{e}(t) = A_{e1}e(t) + D_{e1}w_1(t) \\ e_e(t) = C_{e1}e(t) \end{cases}, \tag{27}$$

where $e^{\mathrm{T}}(t) = \begin{bmatrix} e_x^{\mathrm{T}}(t) & e_d^{\mathrm{T}}(t) & x_r^{\mathrm{T}}(t) \end{bmatrix}, w_1^{\mathrm{T}}(t) = \begin{bmatrix} w^{\mathrm{T}}(t) & \dot{d}^{\mathrm{T}}(t) & r^{\mathrm{T}}(t) \end{bmatrix}$, $A_{e1} = \begin{bmatrix} A_1 + B_1K + \Delta A_1 & B_1 & \Delta A_1 \\ -L\Delta A_1 & -LB_1 & -L\Delta A_1 \\ 0 & 0 & A_r \end{bmatrix}, D_{e1} = \begin{bmatrix} D & 0 & 0 \\ -LD_1 & I & 0 \\ 0 & 0 & B_r \end{bmatrix}$, $C_{e1} = \begin{bmatrix} C_1 & 0 & C_1 \end{bmatrix}$.

Now, a Lyapunov function is chosen as

$$V(t) = e^T(t)\tilde{P}e(t), \tag{28}$$

where $\tilde{P} = diag(P_1, P_2, P_3)$ with $P_i > 0(i = 1,2,3)$. The derivative of $V(t)$ along the closed-loop system Equation (27) is

$$\dot{V}(t) = e^{\mathrm{T}}(t)\left(\tilde{P}A_{e1} + A_{e1}{}^{\mathrm{T}}\tilde{P}\right)e(t) + e^{\mathrm{T}}(t)\tilde{P}D_{e1}\omega_1(t) + \omega_1^{\mathrm{T}}(t)D_{e1}{}^{\mathrm{T}}\tilde{P}e(t). \tag{29}$$

Then, introducing the auxiliary function as

$$J_1(t) = V(t) - \int_0^t w_1^T(s)w_1(s)ds. \tag{30}$$

The initial condition $x(t)$ is assumed to be zero. By using the fact that $V(0) = 0$ and the Equation (30), the term $J_1(t)$ becomes

$$J_1(t) = \int_0^t \left[\dot{V}(s) - w_1^T(s)w_1(s)\right]ds = \int_0^t \tilde{e}^T(s)\Phi\tilde{e}(s)ds, \tag{31}$$

where $\tilde{e}^T(t) = \begin{bmatrix} e^T(t) & w_1^T(t) \end{bmatrix}, \Phi = \begin{bmatrix} A_{e1} + A_{e1}{}^{\mathrm{T}}\tilde{P} + C_{e1}{}^{\mathrm{T}}C_{e1} & \tilde{P}D_{e1} \\ * & -I \end{bmatrix}$.

Using the Lemma 1 and Lemma 2, we can obtain $\tilde{\mathbf{\Phi}} \leq \tilde{\mathbf{\Lambda}}$, and the term $\tilde{\mathbf{\Lambda}}$ has the following form:

$$\tilde{\mathbf{\Lambda}} = \begin{bmatrix} \tilde{\mathbf{\Lambda}}_{11} & P_1B_1 & \mathbf{0} & P_1D_1 & \mathbf{0} & \mathbf{0} \\ * & \tilde{\mathbf{\Lambda}}_{22} & \mathbf{0} & -P_2LD_1 & P_2 & \mathbf{0} \\ * & * & \tilde{\mathbf{\Lambda}}_{33} & \mathbf{0} & \mathbf{0} & P_3B_1 \\ * & * & * & -I & \mathbf{0} & \mathbf{0} \\ * & * & * & * & -I & \mathbf{0} \\ * & * & * & * & * & -I \end{bmatrix}, \tag{32}$$

with

$$\begin{array}{l} \tilde{\mathbf{\Lambda}}_{11} = P_1(A_1 + B_1K_3) + (A_1 + B_1K_3)^{\mathrm{T}}P_1 + \alpha_1 P_1D_2D_2^{\mathrm{T}}P_1 \\ +\alpha_1^{-1}E_1^{\mathrm{T}}E_1 + \alpha_2 P_1D_2D_2^{\mathrm{T}}P_1 + \alpha_3^{-1}E_1^{\mathrm{T}}E_1 \\ \tilde{\mathbf{\Lambda}}_{22} = -P_2LB_1 + (LB_1)^{\mathrm{T}}P_2 + \alpha_4^{-1}P_2LD_2D_2^{\mathrm{T}}L^{\mathrm{T}}P_2 + \alpha_3 P_2LD_2D_2^{\mathrm{T}}L^{\mathrm{T}}P_2 \\ \tilde{\mathbf{\Lambda}}_{33} = P_3A_r + A_r^{\mathrm{T}}P_3 + \alpha_2^{-1}E_1^{\mathrm{T}}E_1 + \alpha_4 E_1^{\mathrm{T}}E_1 \\ \alpha_i(i = 1,2,3,4) > 0 \end{array}.$$

If $\tilde{\mathbf{\Lambda}} < \mathbf{0}$ holds, we have $\tilde{\mathbf{\Phi}} < \mathbf{0}$, i.e., $J_1(t) < \mathbf{0}$. Defining $\tilde{L} = P_2L$ and applying Lemmas 2 and 3 to the inequality $\tilde{\mathbf{\Lambda}} < \mathbf{0}$, we obtain

$$\tilde{\mathbf{\Lambda}}'' = \begin{bmatrix} \tilde{\mathbf{\Lambda}}''_{11} & P_1B_1 & \mathbf{0} & P_1D_1 & \mathbf{0} & \mathbf{0} & \tilde{\mathbf{\Lambda}}''_{17} & \mathbf{0} \\ * & \tilde{\mathbf{\Lambda}}''_{22} & \mathbf{0} & -P_2LD_1 & P_2 & \mathbf{0} & \mathbf{0} & \tilde{\mathbf{\Lambda}}''_{28} \\ * & * & \tilde{\mathbf{\Lambda}}''_{33} & \mathbf{0} & \mathbf{0} & P_3B_r & \mathbf{0} & \mathbf{0} \\ * & * & * & -I & \mathbf{0} & \mathbf{0} & \mathbf{0} & \mathbf{0} \\ * & * & * & * & -I & \mathbf{0} & \mathbf{0} & \mathbf{0} \\ * & * & * & * & * & -I & \mathbf{0} & \mathbf{0} \\ * & * & * & * & * & * & -\tilde{\mathbf{\Lambda}}''_{77} & \mathbf{0} \\ * & * & * & * & * & * & * & -\tilde{\mathbf{\Lambda}}''_{88} \end{bmatrix}, \tag{33}$$

with

$$\begin{array}{l} \tilde{\mathbf{\Lambda}}''_{11} = P_1(A_1 + B_1K_3) + (A_1 + B_1K_3)^{\mathrm{T}}P_1 + \alpha_1^{-1}E_1^{\mathrm{T}}E_1 + \alpha_3^{-1}E_1^{\mathrm{T}}E_1 \\ \tilde{\mathbf{\Lambda}}''_{22} = -P_2LB_1 + (LB_1)^{\mathrm{T}}P_2 \\ \tilde{\mathbf{\Lambda}}''_{33} = P_3A_r + A_r^{\mathrm{T}}P_3 + \alpha_2^{-1}E_1^{\mathrm{T}}E_1 + \alpha_4 E_1^{\mathrm{T}}E_1 \\ \tilde{\mathbf{\Lambda}}''_{17} = \begin{pmatrix} P_1D_2 & P_1D_2 \end{pmatrix} \\ \tilde{\mathbf{\Lambda}}''_{28} = \begin{pmatrix} \tilde{L}D_2 & \tilde{L}D_2 \end{pmatrix} \\ \tilde{\mathbf{\Lambda}}''_{77} = diag(\alpha_1^{-1}I, \alpha_2^{-1}I) \\ \tilde{\mathbf{\Lambda}}''_{88} = diag(\alpha_3^{-1}I, \alpha_4 I) \end{array}.$$

Using the fact that $e_e^T(t)e_e(t) = e^T(t)C_e^TC_ee(t)$ and $J_1(t) < \mathbf{0}$ and invoking Equation (28), if $C_e^TC_e < \gamma^2\tilde{P}$ holds, we have

$$e_e^T(t)e_e(t) < \gamma^2 \int_0^t w_1^T(s)w_1(s)ds. \tag{34}$$

If $w_1(t) = 0$ and $\tilde{\mathbf{\Phi}} < \mathbf{0}$, we have

$$\dot{V}(t) = e^{\mathrm{T}}(t)\left(\tilde{P}A_e + A_e^{\mathrm{T}}\tilde{P}\right)e(t) < 0. \tag{35}$$

Therefore, the augmented closed-loop system Equation (27) is asymptotically stable under the following conditions:

$$\tilde{\mathbf{\Lambda}}'' < \mathbf{0}, C_e^TC_e < \gamma^2\tilde{P}, \tag{36}$$

where $C_e^TC_e < \gamma^2\tilde{P}$ can be further simplified to

$$\begin{bmatrix} C_1^TC_1 - \gamma^2P_1 & \mathbf{0} & C_1^TC_1 \\ \mathbf{0} & -\gamma^2P_2 & \mathbf{0} \\ C_1^TC_1 & \mathbf{0} & C_1^TC_1 - \gamma^2P_3 \end{bmatrix} < 0. \tag{37}$$

Finally, the disturbance observer gain $\boldsymbol{L}$ is obtained as $\boldsymbol{L} = \boldsymbol{P}_2^{-1}\tilde{\boldsymbol{L}}$ by solving the Equations (33) and (37).

In view of the above discussion, the design process of the DOB-based LQR tracking controller is summarized as follows for easy reference:

- Step 1: According to the controlled object in Equation (39) and the reference model system in Equation (40), the gain matrix in the reference model matching controller K_1, K_2 by Assumption 2 is calculated;
- Step 2: Set the LQR weighting matrix $\boldsymbol{Q}, \boldsymbol{R}$; give the prescribed upper bound of LQR performance index γ and the value of input signal $r(t)$; and determine the values of other parameters $D_1, E_1, F_1, \omega(t), d$, etc;
- Step 3: Compute the gain K of the LQR tracking controller by combining Equations (21)–(23);
- Step 4: Compute the gain L of the disturbance observer by combining Equations (33) and (37).

At this point, the LQR-DOB tracking controller design of the electro-optical tracking system with uncertainty and disturbance is completed. Specifically, the disturbance observer is designed as Equation (25) to estimate the disturbances; the reference model matching controller is designed as Equation (14) to track the electro-optical tracking system in Equation (6) with $L_2 - L_\infty$ performance; and the LQR tracking controller is designed as Equation (18).

4. Simulation Analysis and Experimental Verification

4.1. Simulation Analysis

The position transfer function of the controlled object obtained by the electro-optical tracking system through experimental fitting is

$$G(s) = \frac{207}{s^2 + 25.78s + 1151.2}. \tag{38}$$

Convert the above controlled object in Equation (38) into the state-space equation:

$$\begin{aligned} &\begin{bmatrix} \dot{x}_1(t) \\ \dot{x}_2(t) \end{bmatrix} = \begin{bmatrix} 0 & 1 \\ -1151.2 & -25.78 \end{bmatrix} \begin{bmatrix} x_1(t) \\ x_2(t) \end{bmatrix} + \begin{bmatrix} 0 \\ 207 \end{bmatrix} u(t) \\ &y(t) = \begin{bmatrix} 1 & 0 \end{bmatrix} \begin{bmatrix} x_1(t) \\ x_2(t) \end{bmatrix} \end{aligned}, \tag{39}$$

where $x_1(t)$ and $x_2(t)$, respectively, represent the position and speed of the system.

The tracked reference track signal in this paper is generated by the following reference model system, which is shown as

$$\begin{aligned} &\begin{bmatrix} \dot{x}_{r1}(t) \\ \dot{x}_{r2}(t) \end{bmatrix} = \begin{bmatrix} 0 & 1 \\ -4 & -2.828 \end{bmatrix} \begin{bmatrix} x_{r1}(t) \\ x_{r2}(t) \end{bmatrix} + \begin{bmatrix} 0 \\ 1 \end{bmatrix} u(t) \\ &y(t) = \begin{bmatrix} 1 & 0 \end{bmatrix} \begin{bmatrix} x_{r1}(t) \\ x_{r2}(t) \end{bmatrix} \end{aligned}. \tag{40}$$

According to the condition in Assumption 2 and through the above controlled object in Equation (39) and the reference model system in Equation (40), the gain matrix in the reference model matching controller can be obtained as

$$K_1 = \begin{bmatrix} 5.542 & 0.111 \end{bmatrix}, K_2 = 0.0048. \tag{41}$$

Other parameters are given as $D_1 = 0.01\begin{bmatrix} 1 & 1 \end{bmatrix}^T, E_1 = 0.01\begin{bmatrix} 1 & 1 \end{bmatrix}, F_1 = \sin(t)$, $\omega(t) = e^{-5t}, d = \sin(t), Q = \begin{bmatrix} 10 & 0 \\ 0 & 10000 \end{bmatrix}, R = 0.1$, and the upper bound of the LQR performance index $\gamma = 10$ and $r(t) = 1$ is a step signal.

By solving the LMIs in Equations (21)–(24), the gain of the LQR tracking controller is obtained as

$$K = \begin{bmatrix} -0.0596 & -0.003 \end{bmatrix}. \tag{42}$$

By solving the LMIs in Equations (33) and (37), the disturbance observer gain $\boldsymbol{L}$ is obtained as

$$L = \begin{bmatrix} 0.0072 & 0.2924 \end{bmatrix}. \tag{43}$$

In the process of solving the disturbance observer (DOBC) by Equations (33) and (37), the $\tilde{P}$ parameter is shown as

$$P_1 = \begin{bmatrix} 30.2459 & 0.5843 \\ 0.5843 & 0.0377 \end{bmatrix}, P_2 = 31.1002, P_3 = \begin{bmatrix} 17.3446 & 1.1595 \\ 1.1595 & 3.7649 \end{bmatrix}. \tag{44}$$

The eigenvalue of Equation (44) is

$$eig(P_1) = \begin{bmatrix} 0.0264 & 30.2572 \end{bmatrix}^T, eig(P_2) = 31.1002, eig(P_3) = \begin{bmatrix} 3.666 & 17.4429 \end{bmatrix}^T. \tag{45}$$

It can be seen from Equation (45) that the eigenvalue of matrix $\tilde{P}$ is greater than zero, which satisfies the conditions for the LMI method to solve the above inequality relations.

Figure 3 shows the response comparison diagram of the system tracking reference position under sinusoidal disturbance $sin(t)$. The premise parameters such as the LQR weighting matrix $\boldsymbol{Q}, \boldsymbol{R}$, the prescribed upper bound of LQR performance index γ, the value of input signal $r(t)$ and the values of $D_1, E_1, F_1, \omega(t), d$, etc., of all control methods in Figure 3 are guaranteed to be consistent. It can be seen that compared with LQR + DOB with the H_∞ control method, the method proposed in this paper significantly improves the dynamic properties of the system, such as rise time and settling time. The improvement of the dynamic properties of the system is mainly due to the good frequency response characteristics of the LQR tracking controller. Meanwhile, it can be seen that the disturbance observer with $L_2 - L_\infty$ performance index and the model reference tracking controller aim to enhance the robustness and disturbance suppression ability of the system. In addition, it can also be seen in Figure 3 that the gain parameters of DOB observer and controller adjusted by the proposed method are valid. In other words, the LQR tracking control method based on disturbance observer can realize the optimal tracking control of the electro-optical tracking system under the modeling error and uncertain disturbance. This has important practical reference and application value for electro-optical tracking systems.

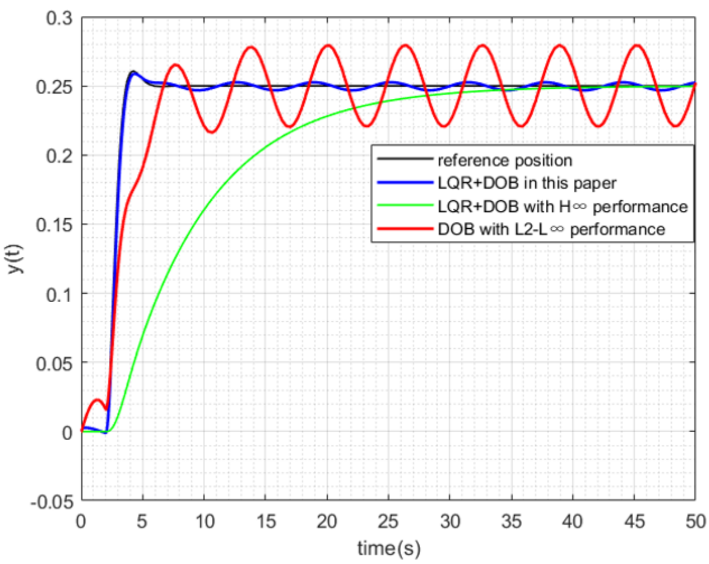

Figure 3. The response comparison diagram of the system tracking reference position under sinusoidal disturbance.

The performance indexes of the tracking reference position of the proposed method in this paper, the LQR + DOB with H_∞ performance control method, and the DOB with $L_2 - L_\infty$ performance control method, such as settling time (T_s) and rise time (T_r), are presented in Table 1 for comparison.

Table 1. Position tracking performance measures.

Method	T_s(s)	T_r(s)
LQR + DOB in this paper	2.97	1.4
LQR + DOB with H_∞ performance	27.36	17.5
DOB with $L_2 - L_\infty$ performance	7.56	4.1

Figure 4 shows the response comparison diagram of the system tracking reference speed under sinusoidal disturbance $sin(t)$. The same conclusion can be drawn from Figure 4 as from Figure 3. Compared with the LQR + DOB with H_∞ control method and the DOB with $L_2 - L_\infty$ control method, the method proposed in this paper significantly improves the dynamic property and disturbance suppression ability of the system. The performance indexes of the tracking reference speed, such as settling time (T_s) and rise time (T_r), are presented in Table 2 for comparison.

Table 2. Speed tracking performance measures.

Method	T_s(s)	T_r(s)
LQR + DOB in this paper	5	2
LQR + DOB with H_∞ performance	34	4.3
DOB with $L_2 - L_\infty$ performance	10.7	2.2

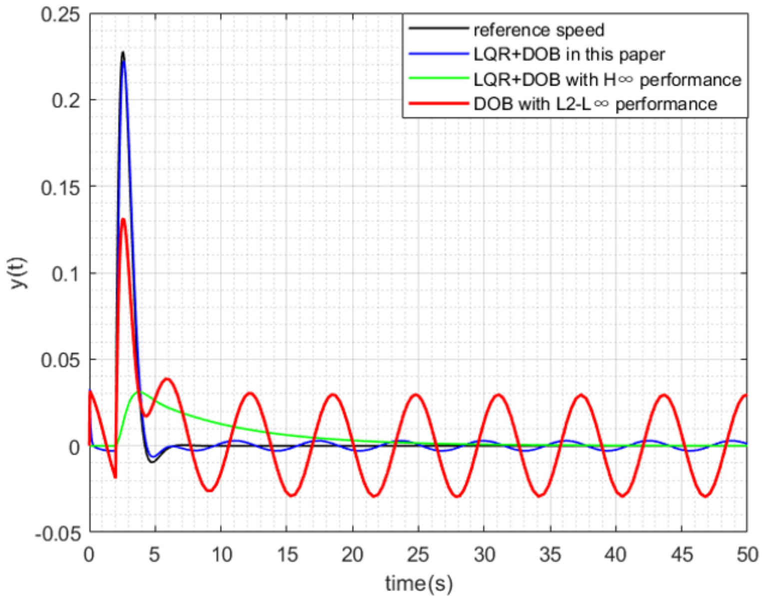

Figure 4. The response comparison diagram of the system tracking reference speed under sinusoidal disturbance.

To sum up, the LQR tracking control method based on disturbance observer can realize the optimal tracking control of the electro-optical tracking system under the modeling error and uncertain disturbance. The LQR tracking controller improves the dynamic response of the system. The model reference tracking controller enhances the robustness of the system. And the DOB with $L_2 - L_\infty$ performance improves the disturbance suppression ability of the electro-optical tracking system. Figure 5 shows the comparison of the disturbance observer under different methods. It can be seen that the DOB under the proposed method can observe the disturbance in real time to compensate. And the disturbance observation progress of the system is relatively high.

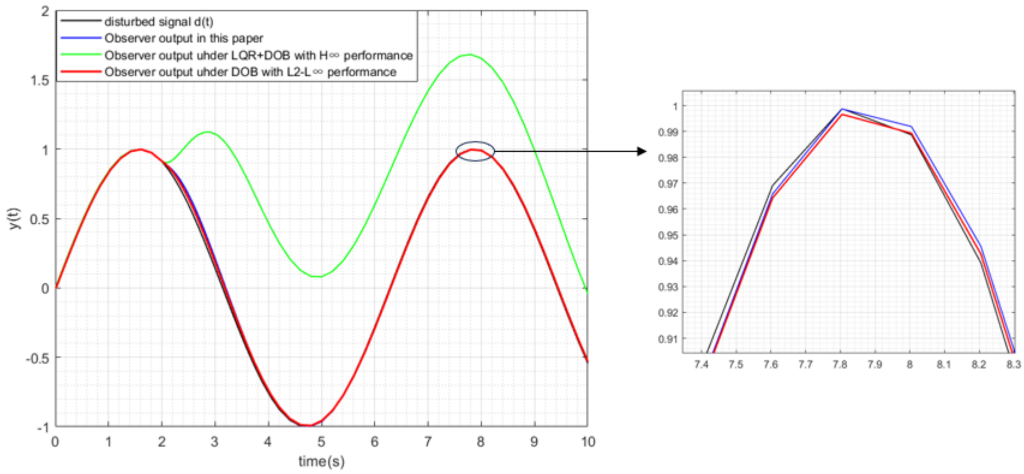

Figure 5. The comparison of disturbance observer under different methods.

4.2. Experimental Verification

To verify the improvement of the dynamic response performance and disturbance suppression ability of the proposed method on the stability control platform, we used the experimental devices shown in Figure 6 for verification.

The electro-optical tracking experimental platform is a two-axis system. This experiment aims at one axis due to the symmetry of the two axes. As shown in Figure 6, the laser light is used to simulate the beacon of light. An apparatus constructed by two superimposed tip-tilt mirror platforms is used to verify the previous analysis. One is used to stabilize the light, and the other is to simulate disturbance, which is measured by position sensors. The electro-optical tracking platform is mounted on the disturbance platform. And both platforms are driven by the voice coil motors. The mirror reflects the laser light into the PSD, which detects the stabilization error at the sampling rate of 5 kHz. In the electro-optical stable tracking system, two main problems need to be solved: one is how to ensure the stability of the optical axis, and the other is the target tracking technology. Stability is a prerequisite for tracking. Therefore, better disturbance suppression ability of the electro-optical platform is conducive to improving the tracking accuracy of the system. The main purpose of this experiment is to verify that the proposed method can significantly improve the disturbance suppression ability and tracking performance of the electro-optical tracking system.

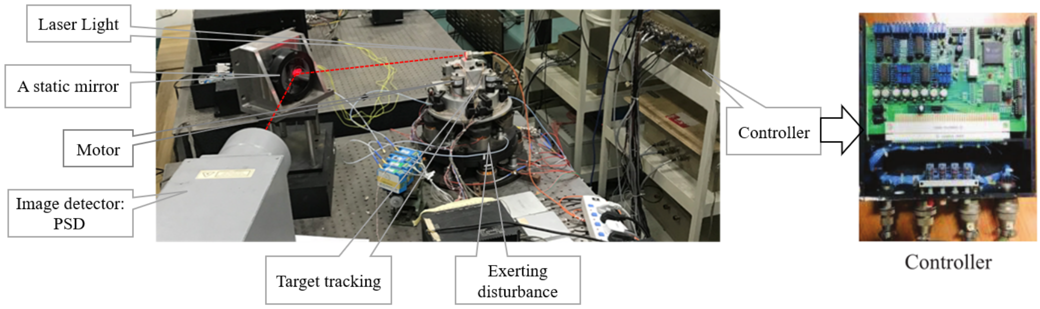

Figure 6. The electro-optical tracking experimental platform.

The disturbed platform is locked when the stable platform is scanned for open-loop position. The characteristic of the electro-optical controlled plant is shown in Figure 7 by inputting the sweep signal to the system. The transfer function of the controlled object obtained by the system identification is as shown in Equation (38). The stability test is to drive the signal to the disturbed platform in the closed loop of the stable platform position and compare the position signal output by the stable platform PSD with that of the disturbed platform.

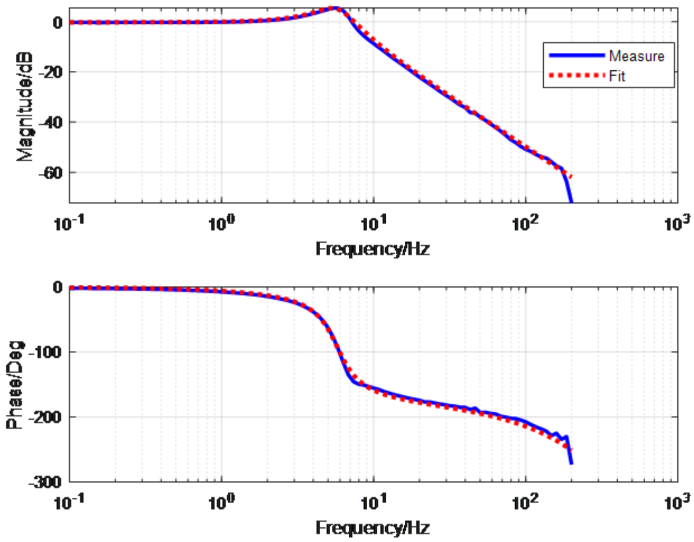

Figure 7. The characteristic of the electro-optical controlled plant.

Firstly, the LQR-DOB tracking control method in this paper is applied to the electro-optical tracking experimental platform. And the disturbance $10sin(t)$ is applied to the disturbance platform. The disturbance input of the electro-optical tracking experimental platform is the value measured by the sensor on the disturbance platform. When the electro-optical tracking platform completes the tracking of the specified target, we simulate the internal disturbance of the electro-optical tracking platform by changing the load on the stable platform. Then, we put a small iron on a stable platform and continue to observe the tracking accuracy and disturbance suppression effect of our control method.

Secondly, the LQR + DOB with H_∞ control method and the DOB with $L_2 - L_\infty$ control method are also applied to the electro-optical tracking experimental platform. In addition, the operation of external disturbance and internal disturbance in the experiment is consistent with the above.

Figure 8 shows the tracking position comparison of the system under different methods. Based on the experimental results, it can be seen that the method proposed in this paper can significantly improve the disturbance suppression ability of the system and dynamic property, such as rise time, settling time and system overshoot. Meanwhile, we can also see that the experimental results are consistent with the above simulation results. The method presented in this paper is effective in the electro-optical tracking system.

Figure 9 shows the tracking speed comparison of the system under different methods. Similarly, compared with the LQR + DOB with H_∞ control method and the DOB with $L_2 - L_\infty$ control method, the method proposed in this paper significantly improves the dynamic property and disturbance suppression ability of the system.

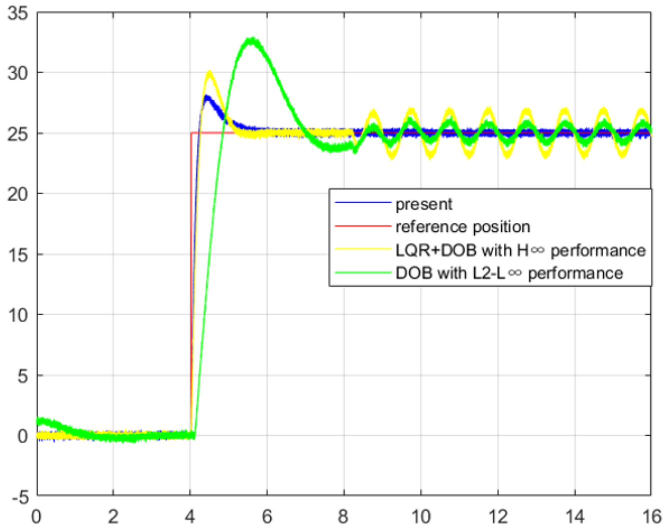

Figure 8. The tracking position comparison of the system under different methods.

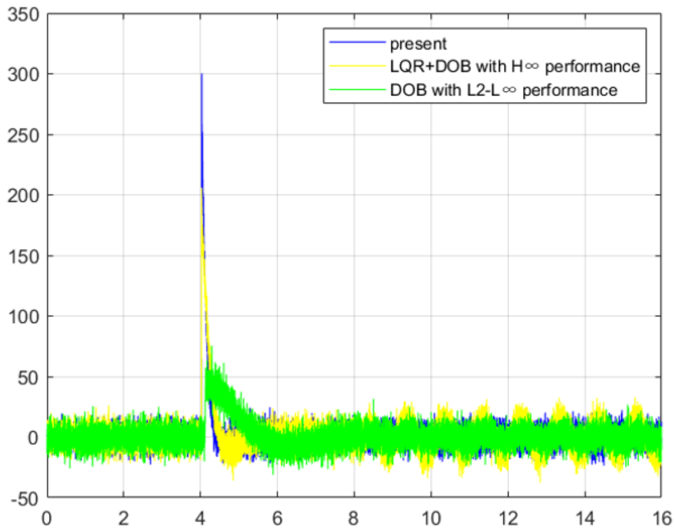

Figure 9. The tracking speed comparison of the system under different methods.

5. Discussion

The LQR-DOB tracking control method proposed in this paper solves the problem of system instability caused by model uncertainty and uncertain disturbance in an electro-optical tracking system. With the increased maneuverability of tracking target, the corresponding control strategy needs to be further studied to achieve the purpose of tracking faster reference signals. From the perspective of control theory, the higher type of control loop has the advantage of tracking faster signals. The design of the high-type control loop has been challenging in academia and industry; that is, it is very difficult to set controller parameters in the high-type control loop. In our future work, high-type control combined with LQR optimal control is introduced into the electro-optical tracking system to improve the disturbance suppression ability, tracking ability and tracking accuracy of the system. In addition, the nonlinear model of the electro-optical tracking system in practical applications can more accurately reflect the characteristics of the system object. Therefore, our future work will focus on designing a nonlinear controller with high-type control combined with optimal control to improve the dynamic response performance of the system and restrain internal and external disturbances. This has a very important application value for electro-optical tracking systems.

6. Conclusions

This paper presents an LQR-DOB tracking control method to solve the problems of modeling error and uncertain disturbance in an electro-optical tracking control system. Using standard techniques, the DOB gain and controller gain of the tracking reference model design is reduced to a convex constraint problem, which can be efficiently solved with the LMI approach. Meanwhile, the stability constraint of the electro-optical tracking closed-loop system is considered by using Lyapunov theory in this framework. Compared with the LQR + DOB with H_∞ control method and the DOB with $L_2 - L_\infty$ control method under the same disturbance condition, the method proposed in this paper can significantly improve the dynamic properties of the system, such as rise time, settling time and system overshoot. The improvement of the dynamic properties of the system is mainly due to the good frequency response characteristics of the LQR tracking controller. Meanwhile, the disturbance observer with $L_2 - L_\infty$ performance index and the model reference tracking controller aim to enhance the robustness and disturbance suppression ability of the system. Specifically, compared with the other methods in this paper, the tracking accuracy and the disturbance suppression ability of the proposed method is about two to three times higher.

However, with the increase in target tracking maneuverability in the electro-optical tracking system, the tracking accuracy and disturbance suppression ability of the system under the proposed method are reduced. To meet the needs of the practical applications of electro-optical tracking systems, the next work of our paper is to further optimize the method in this paper and further solve the problem that the tracking accuracy and disturbance suppression ability of the system decline under the premise of strong tracking target mobility. Meanwhile, many practical constraints, such as controller saturation, will be considered in the next work of this paper. In general, the method proposed in this paper has important reference value for electro-optical tracking systems.

Author Contributions: Conceptualization, C.L., Y.M. and X.Q.; methodology, C.L.; software, C.L. and X.Q.; validation, C.L. and Y.M.; formal analysis, X.Q.; investigation, Y.M.; resources, Y.M.; data curation, X.Q.; writing—original draft, C.L.; writing—review and editing, C.L. and Y.M.; visualization, C.L. and X.Q.; supervision, Y.M.; project administration, Y.M.; funding acquisition, Y.M. All authors have read and agreed to the published version of the manuscript.

Funding: The work described in this article was supported by the National Natural Science Foundation of China (No.61905253).

Informed Consent Statement: Informed consent was obtained from all subjects involved in the study.

Data Availability Statement: The data presented in this study are available from the corresponding author upon reasonable request.

Acknowledgments: The authors sincerely thank the three anonymous reviewers for their valuable comments and suggestions during the peer review process.

Conflicts of Interest: The authors declare no potential conflict of interest with respect to the research, authorship and/or publication of this article.

References

1. Zhou, X.; Li, X. Trajectory tracking control for electro-optical tracking system using ESO based fractional-order sliding mode control. *IEEE Access* **2021**, *9*, 45891–45902. [CrossRef]
2. Zhou, X.; Li, X. Trajectory tracking control for electro-optical tracking system based on fractional-order sliding mode controller with super-twisting extended state observer. *ISA Trans.* **2021**, *117*, 85–095. [CrossRef]
3. Zhao, T.; Tong, W.; Mao, Y. Hybrid Nonsingleton Fuzzy Strong Tracking Kalman Filtering for High Precision Photoelectric Tracking System. *IEEE Trans. Ind. Inform.* **2022**, *19*, 2395–2408. [CrossRef]
4. Duan, Q.; Mao, Y.; Zhang, H.; Xue, W. Add-on integration module-based proportional-integration-derivative control for higher precision electro-optical tracking system. *Trans. Inst. Meas. Control* **2021**, *43*, 1347–1362. [CrossRef]
5. Wang, J.; Guo, Y.; Kong, L.; Rao, C. Experimental demonstration of LQG control with disturbance mitigation on multiple modes in adaptive optics system. *Optik* **2020**, *202*, 163594. [CrossRef]

6. Shi, Q.; Wang, H.; Cheng, H.; Wang, M.; Cheng, F.; Liu, F. Fuzzy disturbance observer-based modified variable gains super-twisting sliding mode composite control for a two-axis airborne optoelectronic stabilized platform. *Optik* **2021**, *228*, 166132. [CrossRef]
7. Wang, J.; Song, Y.; Jiang, H.; Dong, K.; Liu, Y. Prototype development of multi-target tracking system for space multi-node laser communication network. *Optik* **2023**, *274*, 170552. [CrossRef]
8. Deng, J.; Xue, W.; Zhou, X.; Mao, Y. On Dual Compensation to Disturbances and Uncertainties for Inertially Stabilized Platforms. *Int. J. Control Autom. Syst.* **2022**, *20*, 1521–1534. [CrossRef]
9. Zhang X, Wang J. Multi-loop Feedback Analysis of Distributed Power Inverters in Microgrids. In Proceedings of the 2023 IEEE International Conference on Control, Electronics and Computer Technology (ICCECT), Jilin, China, 28–30 April 2023; IEEE: Piscataway, NJ, USA, 2023; pp. 1431–1434.
10. Deng, J.; Xue, W.; Liang, W.; Zhou, X.; Mao, Y. On adjustable and lossless suppression to disturbances and uncertainties for nonminimum-phase laser pointing system. *ISA Trans.* **2023**, *136*, 727–741. [CrossRef]
11. Toor, W.A.; Ashraf, M. Performance Analysis of Learning-Based Disturbance Observer for Pulsed Superconducting Cavity Field Control. *Electronics* **2023**, *12*, 1556. [CrossRef]
12. Lubing, X.; Yangfei, Y.; Yang, Y.;Weixing, Z. DOB Tracking Control Algorithm for Unmanned Aerial Vehicles with TS Disturbance Modeling. In Proceedings of the 2021 40th Chinese Control Conference (CCC), Shanghai, China, 26–28 July 2023; IEEE: Piscataway, NJ, USA, 2021; pp. 503–508.
13. Grunwald, R.; Jurke, M.; Bock, M.; Liebmann, M.; Bruno, B.P.; Gowda, H.; Wallrabe, U. High-flexibility control of structured light with combined adaptive optical systems. *Photonics* **2022**, *9*, 42. [CrossRef]
14. Pochechuev, M.S.; Fedotov, I.V.; Solotenkov, M.A.; Andreeva, M.S.; Lanin, A.A.; Fedotov, A.B.; Zheltikov, A.M. Adaptive Wave-Front Shaping and Beam Focusing through Fiber Bundles for High-Resolution Bioimaging. *Photonics* **2021**, *9*, 21. [CrossRef]
15. Abbasi, A.; Moshayedi, A.J. Trajectory tracking of two-wheeled mobile robots, using LQR optimal control method, based on computational model of KHEPERA IV. *J. Simul. Anal. Nov. Technol. Mech. Eng.* **2018**, *10*, 41–50.
16. Liu, C.; Duan, Q.; Zhang, C.; Luo, Y.; Qiu, X.; Xia, W.; Li, H.; Mao, Y. Extending the LQR to the design of PID type-ii and type-iii control loops. *IET Control Theory Appl.* **2023**, *17*, 713–743. [CrossRef]
17. Okasha, M.; Kralev, J.; Islam, M. Design and Experimental Comparison of PID, LQR and MPC Stabilizing Controllers for Parrot Mambo Mini-Drone. *Aerospace* **2022**, *9*, 298. [CrossRef]
18. Elkhatem, A.S.; Engin, S.N. Robust LQR and LQR-PI control strategies based on adaptive weighting matrix selection for a UAV position and attitude tracking control. *Alex. Eng. J.* **2022**, *61*, 6275–6292. [CrossRef]
19. Bilgic, H.H.; Sen, M.A.; Yapici, A.; Yavuz, H.; Kalyoncu, M. Meta-heuristic tuning of the LQR weighting matrices using various objective functions on an experimental flexible arm under the effects of disturbance. *Arab. J. Sci. Eng.* **2021**, *46*, 7323–7336. [CrossRef]
20. Németh, Z.; Kuczmann, M. Linear-Matrix-Inequality-Based Controller and Observer Design for Induction Machine. *Electronics* **2022**, *11*, 3894. [CrossRef]
21. Kim, Y.; Tran, T.V.; Kim, K.H. LMI-based model predictive current control for an LCL-filtered grid-connected inverter under unexpected grid and system uncertainties. *Electronics* **2022**, *11*, 731. [CrossRef]
22. Gritli, H.; Zemouche, A.; Belghith, S. On LMI conditions to design robust static output feedback controller for continuous-time linear systems subject to norm-bounded uncertainties. *Int. J. Syst. Sci.* **2021**, *52*, 12–46. [CrossRef]
23. Feng, Z.Y.; Guo, H.; She, J.; Xu, L. Weighted sensitivity design of multivariable PID controllers via a new iterative LMI approach. *J. Process Control* **2022**, *110*, 24–34. [CrossRef]
24. Wang, X.; Chen, X.; Wen, L. The LQR baseline with adaptive augmentation rejection of unmatched input disturbance. *Int. J. Control Autom. Syst.* **2017**, *15*, 1302–1313. [CrossRef]
25. Duan, G.R.; Yu, H.H. *LMIs in Control Systems: Analysis, Design and Applications*; CRC Press: Boca Raton, FL, USA, 2013.
26. Li, Y.; Sun, H.; Zong, G.; Hou, L. Anti-disturbance control for time-varying delay Markovian jump nonlinear systems with multiple disturbances. *Int. J. Syst. Sci.* **2017**, *48*, 3186–3200. [CrossRef]